AIP | Applied Physics Letters

Tunneling-enabled spectrally selective thermal emitter based on flat metallic films

Zhu Wang, Ting Shan Luk, Yixuan Tan, Dengxin Ji, Ming Zhou, Qiaoqiang Gan, and Zongfu Yu

Citation: Applied Physics Letters **106**, 101104 (2015); doi: 10.1063/1.4914886
View online: http://dx.doi.org/10.1063/1.4914886
View Table of Contents: http://scitation.aip.org/content/aip/journal/apl/106/10?ver=pdfcov
Published by the AIP Publishing

Tunneling-enabled spectrally selective thermal emitter based on flat metallic films

Zhu Wang,[1] Ting Shan Luk,[2,a)] Yixuan Tan,[1] Dengxin Ji,[3] Ming Zhou,[1] Qiaoqiang Gan,[3] and Zongfu Yu[1,b)]
[1]*Department of Electrical and Computer Engineering, University of Wisconsin-Madison, Wisconsin 53706, USA*
[2]*Center for Integrated Nanotechnologies (CINT), Sandia National Laboratories, Albuquerque, New Mexico 87185, USA*
[3]*Department of Electrical and Computer Engineering, New York State University of Buffalo, Buffalo, New York 14260, USA*

(Received 5 February 2015; accepted 3 March 2015; published online 11 March 2015)

Infrared thermal emission from metals has important energy applications in thermophotovoltaics, radiative cooling, and lighting. Unfortunately, the emissivity of flat metal films is close to zero because the screening effect prevents metals' fluctuating currents from emitting to the far field. As a result, metal films are often used as reflecting mirrors instead of thermal emitters. Recently, nanostructured metals, such as metamaterials, have emerged as an interesting way to enhance and to spectrally control thermal emission based on plasmonic resonant effects. However, they require sophisticated lithography. Here, we proposed and experimentally demonstrated a completely different mechanism to achieve spectrally selective metallic emitters based on a tunneling effect. This effect allows a simple flat metal film to achieve a near-unity emissivity with controlled spectral selectivity for efficient heat-to-light energy conversion. © *2015 AIP Publishing LLC*.
[http://dx.doi.org/10.1063/1.4914886]

A blackbody radiates in a wide spectral range. Such broadband emission is often undesirable in many energy applications that rely on radiative heat as the primary mode of energy exchange. For example, in thermophotovoltaics, an ideal emitter should have a sharp cut-off in the near-infrared spectral range.[1–3] In passive radiative cooling,[4] the emitter should only radiate in wavelength range between 8 and 13 μm.[5] Driven by these energy applications, there has been a great amount of recent interests in spectrally selective thermal emitters.[6–13]

There are two approaches to achieve the spectral selectivity. The first relies on the intrinsic dielectric property of materials. For example, SiC is used for thermal emission in the selected spectral range between 10 and 13 μm[14] based on its phonon polaritons. Generally, this approach requires minimal amount of nanofabrication because the spectral selectivity is offered by the intrinsic properties of the material. The main drawback is the lack of spectral tunability and potential material incompatibility. The second approach is based on nanostructured materials.[15,16] This approach offers greater flexibility in tuning the emission spectra because the spectral features are determined by the structure instead of any intrinsic dielectric properties. Metals are often the favorite choice of materials because they can be made to selectively emit at any wavelength from visible to THz.[17,18] This capability is enabled by the fact that metals' thermal emission mainly comes from free carriers instead of transitions in quantized energy levels. However, due to the strong screening effect, a flat metal film has very low emissivity. To overcome such issue, recently metamaterial emitters have emerged as a very interesting solution based on the plasmonic resonances of metals. A variety of metallic structures have been demonstrated, including nanoparticles, gratings, and hyperbolic metamaterials,[19–24] to name a few. Despite its great spectral tunability, using nanostructures to control emission imposes a significant barrier for practical applications because it often requires expensive lithography. It is therefore highly desirable to achieve spectrally selective emitters without nanostructure patterning. In this paper, we report a spectral selective emitter based on flat metallic films. Instead of plasmonic resonance, we rely on the tunneling effect in extremely thin films. The tunneling effect enhances the emissivity of metal film over extremely broadband range. A simple Fabry-Perot cavity can be used to accomplish the spectral selectivity. This method allows the large-area low-cost fabrication of spectrally selective thermal emitter, which could be used in a variety of energy applications.

Metals have great potential to become efficient thermal emitters because of their high density of free charges. This potential is also reflected by the large value of the imaginary part of the dielectric constant, particularly in the infrared regime. However, the strong screening effect prevents the fluctuating currents inside the metal from radiating to the free space. As a result, flat metal films typically have a low emissivity below 5%. To illustrate such screening effect in simulations, Figure 1(a) shows the emission by an electric-current point source, which can be considered as the building element of a thermal source. The point source emitting at a wavelength of 10 μm is placed 0.5 nm below the air-silver interface, a distance much shorter than the skin depth (~10 nm for silver). The simulation is performed by solving the Maxwell's equations with a finite-element method. The dielectric constant of silver is taken from Ref. 25. One can

a)Email: tsluk@sandia.gov
b)Email: zyu54@wisc.edu

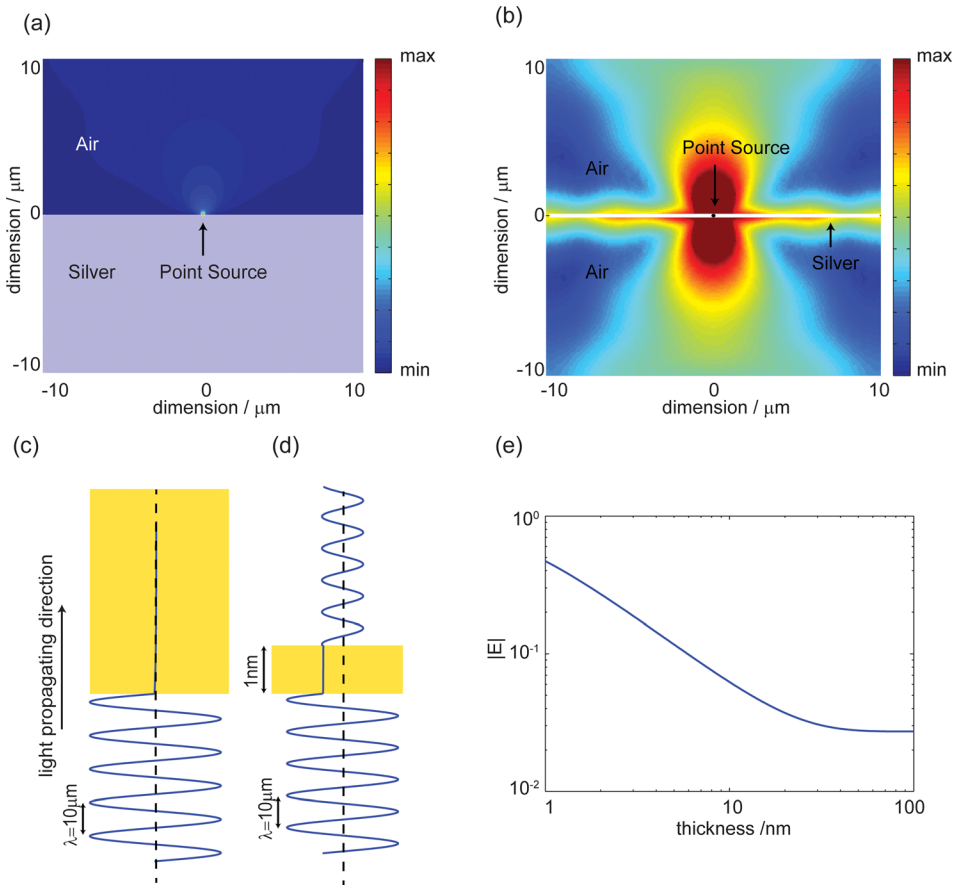

FIG. 1. (a) Radiation by an electric-current point source placed 0.5 nm below the interface between air and a semi-infinite silver slab. (b) Radiation by an electric-current point source placed in the center of a 1-nm-thick silver film. (c) and (d) Electric field distributions of light incident normally upon a semi-infinite silver slab (c) and a 1-nm-thick silver film (d). (e) The strength of the electric field at the air-silver interface for silver films of different thickness. The incident field $|E_0| = 1$.

see that despite being close to the surface, the point source radiates weakly. The bulk Ag material below the point current effectively prevents the far-field emission. Conventional approaches of enhancing the emission in metals exploit the plasmonic resonances in nanostructures, such as metamaterial emitters, which inevitably requires nano-patterning. Here, we explore a completely different mechanism based on the tunneling effect in flat and continuous ultra-thin metal films. To briefly illustrate the idea, Figure 1(b) shows the same current source placed in the center of a 1-nm-thick silver film. Due to the thin thickness, the film does not have enough charges to screen the oscillating current. The emission is drastically enhanced in ultra-thin flat film, which can be directly visualized by comparing Figures 1(a) and 1(b), where the same color map is used. Moreover, unlike the plasmonic resonant enhancement, the tunneling enhancement is a non-resonant effect, meaning that it has extremely broad spectral bandwidth. The classical model studied here does not include the effect of quantum plasmon,[26] which could introduce additional correction without affecting the main conclusion.

The enhanced emission can also be understood by considering the light absorption of ultra-thin films because the absorption is the reciprocal process of thermal emission. The absorption by a material is linearly proportional to both the imaginary part of the dielectric constant ϵ_{img} and the intensity of electric field $|E|^2$ inside the material. Metals normally have very large ϵ_{imag} in the infrared spectral range. But the electric field inside metals is extremely weak when light shines on a thick metal slab. The electric field can be described as $E\exp[2\pi(-i\,n-k)x/\lambda]$, where n and k are the real and imaginary parts of the refractive index of the metal, respectively. Normally, k is much larger than n for infrared light. The amplitude $|E| \approx 2|E_0|/k$, where E_0 is the amplitude of the incident light. As an example, $n = 7$ and $k = 73$ for silver at the wavelength of 10 μm, resulting in an amplitude $|E|$ that is only 2.7% of the incident field $|E_0|$. Figure 1(c) shows the field distribution for a light normally incident upon a thick slab, where the field goes to nearly zero instantaneously in the metal. The resulting absorption and emissivity is extremely weak despite silver's large ϵ_{img} value. On the other hand, for ultra-thin films of a few nm thickness, metals are no longer good mirrors, which allow photons to tunnel through. The electric field strength inside the metal is significantly enhanced. In the infrared regime, where the wavelength $\lambda \sim 10^3 - 10^4$ nm, the film thickness $d/\lambda \ll 1$ and the amplitude inside the film are comparable to the incident field. Figure 1(d) shows the field distribution for light tunneling through a 1-nm-thick Ag film. The amplitude $|E| = 47\%|E_0|$. Figure 1(e) shows the simulated values of $|E|$ for films of different thicknesses. The tunneling effect is most prominent when the thickness is below 10 nm. As the thickness increases, the tunneling becomes weaker and the amplitude of the field inside silver decreases. When the d is thick enough, e.g., thicker than a few tens of nm, we can treat it as a bulk metal and $|E|$ becomes a small constant independent of the film thickness. Therefore, to obtain an enhanced electric field inside the metal, an ultra-thin film is desired where its absorption and thermal emission can be enhanced.

Figure 2(a) compares the spectra of the emissivity of a thick (dashed) and a 1-nm-thick (dotted) silver film in the

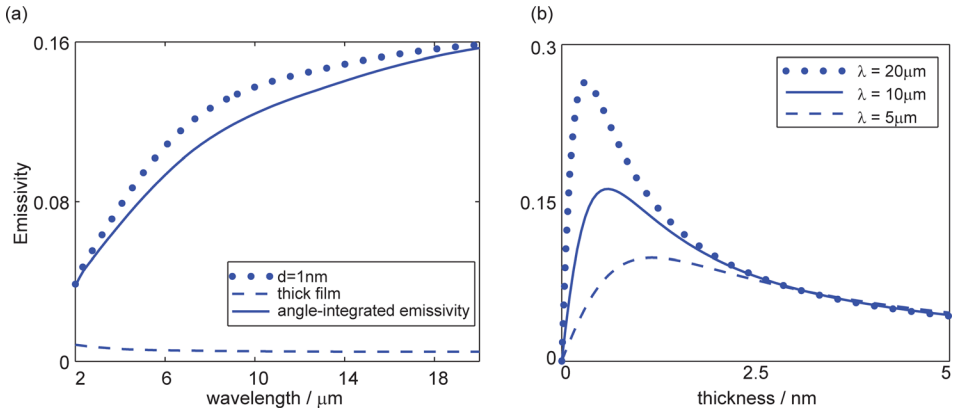

FIG. 2. (a) Dotted line: the emissivity of the 1 nm silver film in the direction normal to the surface; dashed line: the emissivity of a bulk silver slab in the normal direction; solid line: the angle-integrated emissivity of 1 nm silver film. (b) The emissivity as a function of the thickness of the ultra-thin silver film at the wavelengths of 5 μm (dashed), 10 μm (solid), and 20 μm (dotted).

direction normal to the surface. One can see that the emissivity of the thick film is always less than 1% in the infrared regime. In great contrast, the emissivity of the 1-nm-thick film is up to 16%. More importantly, the emissivity is enhanced over an extremely broad range of spectrum because the tunneling effect does not rely on any optical resonance.

The enhancement due to the tunneling effect is not sensitive to the direction of the thermal emission. To evaluate the total thermal emission in all angles, we calculated the angle-integrated emissivity defined by

$$e_T = \frac{1}{2}\sum_{s,p}\frac{1}{\pi}\int_0^{\pi/2} d\theta \int_0^{2\pi} d\varphi e(\theta,\varphi)\cos(\theta)\sin(\theta),$$

where $e(\theta,\varphi)$ is the angle-dependent emissivity. The summation is performed for the two polarization states s and p. The result for the 1-nm-thick film is shown by the solid line in Figure 2(a). It is almost the same as the emissivity in the normal direction, indicating excellent isotropic emission.

The tunneling effect leads to stronger fields in the metal when we reduce the thickness of a film. However, the emissivity will not grow monotonically with a decreasing thickness because the thermal emission also scales with the volume of the materials. For example, for the wavelength of 10 μm, a maximum emissivity of 16.3% is achieved when the film is 0.6 nm thick. Figure 2(b) shows the dependence of emissivity on the thickness of the silver film for the wavelengths of 5 μm (dashed), 10 μm (solid), and 20 μm (dotted). They all reach peak emissivity at certain finite thicknesses.

Another interesting trend can be identified in Figures 2(a) and 2(b): ultra-thin films emit more thermal energy in the longer wavelength range. This trend is somewhat counterintuitive, considering that silver slabs are considered as better mirrors and weaker emitters in the longer wavelength range. Here, in ultra-thin films, the amplitude of the field inside metals is on the same scale for different wavelengths, owing to the tunneling effect. However, the imaginary part of the dielectric constant ε_{imag} increases when the wavelength increases, resulting in stronger thermal emission in the long wavelength range.

Figs. 1 and 2 show that the tunneling effect in ultra-thin films can enhance the emissivity over extremely broad spectral range. To achieve spectral selectivity, the simplest approach is to use a Fabry-Perot cavity in a salisbury screen design,[27,28] as shown in Figure 3(a). The cavity consists of three layers: a thick Ag layer as the bottom mirror, a Si layer as the transparent spacer, and an ultra-thin Ag film as the active thermal emitter. The resonance of this cavity further enhances the emissivity at the resonant frequency and suppresses the emissivity at off-resonant frequencies. The wavelength of the emission is primarily determined by the thickness of the spacer.

Figure 3(b) shows the calculated emissivity for different Si spacer thicknesses. The thickness of the silver film is 2 nm. The emissivity is close to unity around the resonant wavelengths. The resonant wavelengths increase as the spacer thickness increases. Higher order cavity modes start to appear with a thicker spacer. As an example, to achieve a selective emitter at the wavelength of 10 μm, we choose a Si spacer of 1.22 μm thick. For a 2-nm-thick top layer of silver, the peak emissivity reaches 98.2% (Figure 3(c) dashed line). The bandwidth of the selective emitter can also be tuned. The bandwidth is primarily determined by the reflectivity of the top silver film and the length of the cavity. A thinner film leads to a weaker reflectivity and a broader bandwidth. A longer cavity leads to higher quality factor and thus narrower bandwidth. As an example, when we reduce the thickness of the silver film from 2 nm to 1 nm, the emission bandwidth is significantly broadened (Figure 3(c) solid line). The cavity also preserves the angular response of ultra-thin film very well. The emissivity for different emission angles at the wavelength of 10 μm is plotted in Figure 3(d), showing high emissivity for broad angular response and for both polarization states.

Next, we experimentally demonstrate spectrally selective emitters based on ultra-thin flat films. We started with a Si substrate with root-mean-square (RMS) roughness of $<$0.02 nm. Silver films were deposited on Si substrates with a 1-nm-thick Ge film as the wetting layer using electronic beam evaporation. The deposition rate is set to 0.1 A/s to control the thickness accurately. The slow deposition rate is important to minimize roughness growth. All films were deposited at room temperature with electron beam thermal evaporation with a typical base pressure of 5×10^{-7} Torr. A 100-nm-thick Ag mirror layer is followed by an 870-nm-thick amorphous silicon layer and finally a 3-nm-thick Ag film. Figure 4(e) shows the photo of a fabricated sample.

This 3-nm-thick Ag film was also deposited on a control glass sample for spectroscopic ellipsometry characterization, which is used to confirm the thickness of the deposited Ag. The thickness and optical constants of the film are fitted in the spectral region from 0.285 to 1 μm. The ellipsometry fit was obtained using Drude model and Tauc-Lorentz

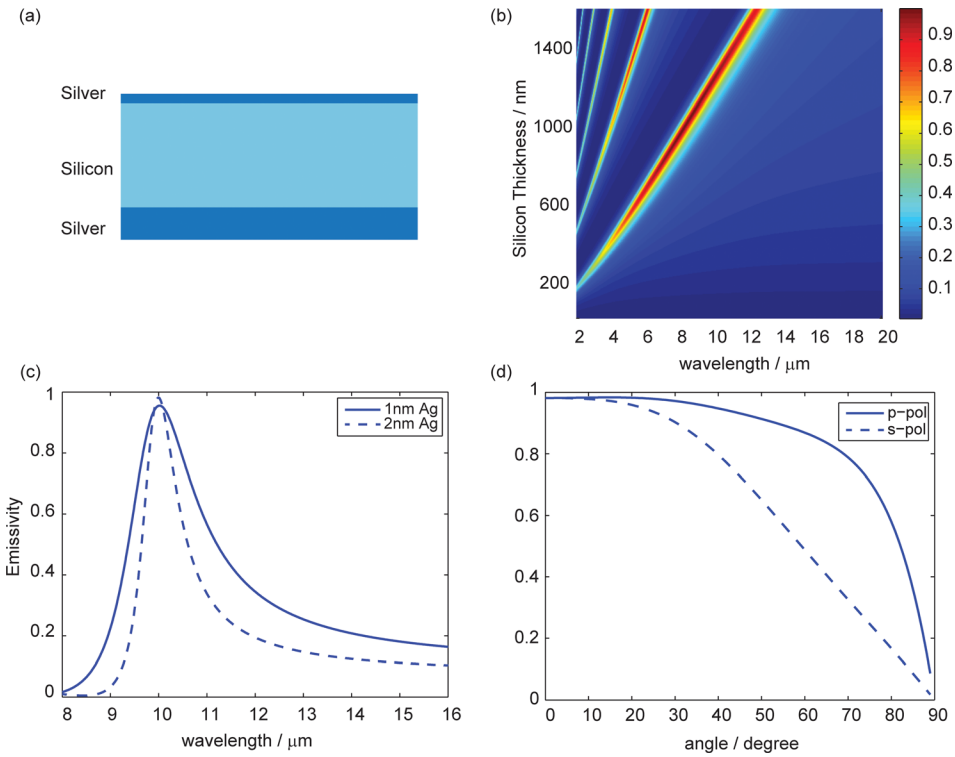

FIG. 3. (a) The structure of the cavity. (b) The emissivity of the top layer 2 nm silver in this cavity as a function of both wavelength and Si thickness. (c) The emissivity of the cavity as a function of wavelength. Dashed line: the emissivity of the cavity with 2 nm Ag on top and 1227 nm Si in between; solid line: the emissivity of the cavity with 1 nm Ag on top and 1077 nm Si in between. (d) The emissivity of the top layer 1 nm silver as a function of incident angle at $\lambda = 10\,\mu$m. Dashed (solid) line is for s (p) polarized light.

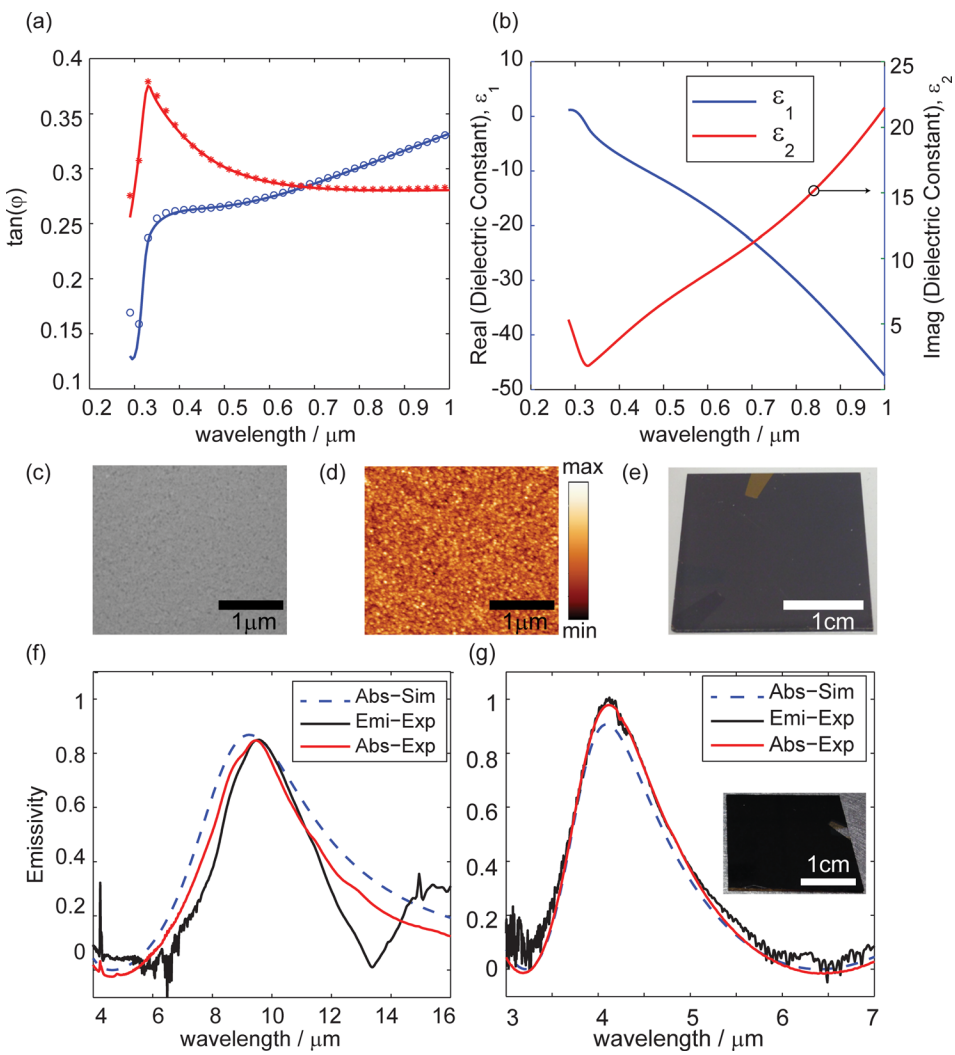

FIG. 4. (a) Spectroscopic ellipsometry parameter tan(φ) for a ultra-thin Ag film on a glass substrate. Measured values for incident angles of 60° and 70° are shown by the open-circle and star markers, respectively. The solid lines are the fitted value based on Drude model and Tauc-Lorentz oscillator. (b) Fitted dielectric constants of the silver film. Blue and red curves represent the real and imaginary parts of the dielectric constant, respectively. (c)–(e) SEM (c) image, AFM (d) image, and photography (e) of the sample. (f) Measured emissivity (black line) and absorption (red line) for the spectrally selective emitter. Dashed line is the simulated absorption. (g) Tuning the emission frequency by varying the length of the cavity. The measured emissivity (black solid), measured absorption (red solid), and the simulated absorption for a cavity with a Si spacer that is 874 nm thick. The top layer is 3 nm thick silver. The inset shows the photograph of the fabricated sample.

oscillator, which is used to describe the interband absorption in the UV spectral region. Figure 4(a) shows the measured ratio $\tan(\Psi) = |\frac{r_p}{r_s}|$ between the reflected amplitudes of s and p polarization lights. Excellent fitted curves are obtained for two different incident angles. The thickness was determined to be 3 nm, agreeing perfectly with our pre-set deposited thickness. The fitted dielectric constants are shown in Figure 4(b).

Sharp rise in curves shown in Figure 4(a) in the short wavelength is a result of sharp transition of dielectric to metallic behavior, a good indicator of high quality silver film. Moreover, the lack of pronounced drop in the spectral feature shown in Figure 4(a) provides evidences that the film can be considered continuous. There is also no hint of localized surface plasmon absorption feature in the visible region caused by islanding effect of Ag film. The continuity of the thin film is also supported by the atomic force microscopy (AFM) and scanning electron microscope (SEM) measurements shown by Figures 4(c) and 4(d). The SEM image of the top surface indicates the excellent flatness of the surface of a continuous ultra-thin metal film. The RMS roughness measured in the AFM is 0.8 nm, much smaller than the film thickness of 3 nm.

For the characterization of the thermal emission, we employ a heating stage (Linkam, TS1500) installed in a Fourier Transform Infrared spectroscopy (FTIR, Bruker Vertex 70) to accurately control the temperature of the sample. The sample is heated to 100 °C in the chamber filled with nitrogen. In order to calculate the emissivity, an area of the emitter is coated with carbon black[29] which has very high emissivity (i.e., ~0.9 of ideal blackbody emissivity) and is used as the normalization reference. By having the black carbon on the emitter directly, we ensure that it is at the same temperature as our selective emitter. A FTIR microscope (Bruker, Hyperion 1000) is used to selectively characterize different regions of the sample with the area of 400 μm × 400 μm.

Figure 4(f) shows the experimentally measured emissivity for a cavity with a 653 nm thick Si spacer. The emissivity has a peak value close to unity at the wavelength around 9 μm. The emission is suppressed away from the resonant frequency. The Fabry-Perot cavity works very well for the spectral selectivity. The simulation based on fitted dielectric constants is shown by dashed line in Figure 4(f), which agrees very well the experiment. The emissivity also agrees very well with the measured absorption of the sample, which is indicated by the red solid line.

Thus, we can easily tune the wavelength of thermal emission by controlling the thickness of Si slab. For this purpose, we fabricate another cavity with an 874-nm-thick Si spacer and a 3-nm-thick silver film. The same characterization is performed. The results are shown in Figure 4(g). The wavelength of the second order Fabry-Perot mode is around 4 μm. Indeed, we observe enhanced thermal emission at this wavelength with an emissivity close to unity. The measured absorption agree very well with the measured emissivity as well as simulation result.

In conclusion, large-area spectrally selective thermal emitters are a critical component in energy conversion applications. The existing methods based on metamaterial metallic structures are not suitable for low-cost large-area applications because of the expensive lithography processes. Here, we proposed and experimentally demonstrated an emission mechanism based on the tunneling effect, which enables a flat metallic film to efficiently emit thermal energy at selected wavelengths. Without involving any nano patterning, the tunneling-enabled emission offers an extremely simple and low-cost method to obtain large area spectrally selective emitters.

The authors acknowledge the initial experimental help from Dr. Iltai Kim. The work was partially supported by National Science Foundation (Nos. ECCS-1405201 and ECCS-1425648). This work was performed, in part, at the Center for Integrated Nanotechnologies, an Office of Science User Facility operated for the U.S. Department of Energy (DOE) Office of Science. Sandia National Laboratories is a multi-program laboratory managed and operated by Sandia Corporation, a wholly owned subsidiary of Lockheed Martin Corporation, for the U.S. Department of Energy's National Nuclear Security Administration under Contract No. DE-AC04 94AL85000.

[1]A. Narayanaswamy and G. Chen, Appl. Phys. Lett. **82**, 3544 (2003).
[2]E. Rephaeli and S. Fan, Opt. Express **17**, 15145 (2009).
[3]A. Lenert, D. M. Bierman, Y. Nam, W. R. Chan, I. Celanović, M. Soljačić, and E. N. Wang, Nat. Nanotechnol. **9**, 126 (2014).
[4]A. P. Raman, M. A. Anoma, L. Zhu, E. Rephaeli, and S. Fan, Nature **515**, 540 (2014).
[5]E. Rephaeli, A. Raman, and S. Fan, Nano Lett. **13**(4), 1457 (2013).
[6]M. U. Pralle, N. Moelders, M. P. McNeal, I. Puscasu, A. C. Greenwald, J. T. Daly, E. A. Johnson, T. George, D. S. Choi, I. El-Kady, and R. Biswas, Appl. Phys. Lett. **81**, 4685 (2002).
[7]S. Y. Lin, J. Moreno, and J. G. Fleming, Appl. Phys. Lett. **83**, 380 (2003).
[8]M. Laroche, C. Arnold, F. Marquier, R. Carminati, J.-J. Greffet, S. Collin, N. Bardou, and J.-L. Pelouard, Opt. Lett. **30**, 2623 (2005).
[9]M. Laroche, R. Carminati, and J.-J. Greffet, Phys. Rev. Lett. **96**, 123903 (2006).
[10]P. Nagpal, S. E. Han, A. Stein, and D. J. Norris, Nano Lett. **8**, 3238 (2008).
[11]J. A. Schuller, T. Taubner, and M. L. Brongersma, Nat. Photonics **3**, 658 (2009).
[12]M. De Zoysa, T. Asano, K. Mochizuki, A. Oskooi, T. Inoue, and S. Noda, Nat. Photonics **6**, 535 (2012).
[13]B. J. Lee, C. J. Fu, and Z. M. Zhang, Appl. Phys. Lett. **87**, 071904 (2005).
[14]N. Landy, S. Sajuyigbe, J. Mock, D. Smith, and W. Padilla, Phys. Rev. Lett. **100**, 207402 (2008).
[15]N. Liu, M. Mesch, T. Weiss, M. Hentschel, and H. Giessen, Nano Lett. **10**, 2342 (2010).
[16]M.-W. Tsai, T.-H. Chuang, C.-Y. Meng, Y.-T. Chang, and S.-C. Lee, Appl. Phys. Lett. **89**, 173116 (2006).
[17]O. D. Miller, S. G. Johnson, and A. W. Rodriguez, Phys. Rev. Lett. **112**, 157402 (2014).
[18]S. Shen, A. Mavrokefalos, P. Sambegoro, and G. Chen, Appl. Phys. Lett. **100**, 233114 (2012).
[19]G. E. Jellison and F. A. Modine, Appl. Phys. Lett. **69**, 371 (1996).
[20]J. Hao, L. Zhou, and M. Qiu, Phys. Rev. B **83**, 165107 (2011).
[21]K. Aydin, V. E. Ferry, R. M. Briggs, and H. A. Atwater, Nat. Commun. **2**, 517 (2011).
[22]C. Wu, B. Neuner III, J. John, A. Milder, B. Zollars, S. Savoy, and G. Shvets, J. Opt. **14**, 024005 (2012).
[23]Y. Cui, K. H. Fung, J. Xu, H. Ma, Y. Jin, S. He, and N. X. Fang, Nano Lett. **12**, 1443 (2012).
[24]H. Hu, D. Ji, X. Zeng, K. Liu, and Q. Gan, Sci. Rep. **3**, 1249 (2013).
[25]H.-J. Hagemann, W. Gudat, and C. Kunz, JOSA **65**, 742 (1975).
[26]J. A. Scholl, A. L. Koh, and J. A. Dionne, Nature **483**, 421 (2012).
[27]M. S. Jang, V. W. Brar, M. C. Sherrott, J. J. Lopez, L. Kim, S. Kim, M. Choi, and H. A. Atwater, Phys. Rev. B **90**, 165409 (2014).
[28]K. T. Jonathan, W. C. Hsu, Y. Huang, S. V. Boriskina, and G. Chen, "Thin-film 'Thermal Well' Emitters and Absorbers for High-Efficiency Thermophotovoltaics," e-print arXiv:1502.02061.
[29]Z. Yu, N. P. Sergeant, T. Skauli, G. Zhang, H. Wang, and S. Fan, Nat. Commun. **4**, 1730 (2013).